



## Finite Elements Based on Strong and Weak Formulations for Structural Mechanics: Stability, Accuracy and Reliability

†Francesco Tornabene<sup>1</sup>, Nicholas Fantuzzi<sup>1</sup>, and Michele Bacciocchi<sup>1</sup>

<sup>1</sup>DICAM - Department, University of Bologna, Viale del Risorgimento 2, 40136 Bologna, Italy  
†E-mail address: [francesco.tornabene@unibo.it](mailto:francesco.tornabene@unibo.it)

Received date: April 2017

### Abstract

The authors are presenting a novel formulation based on the Differential Quadrature (DQ) method which is used to approximate derivatives and integrals. The resulting scheme has been termed strong and weak form finite elements (SFEM or WFEM), according to the numerical scheme employed in the computation. Such numerical methods are applied to solve some structural problems related to the mechanical behavior of plates and shells, made of isotropic or composite materials.

The main differences between these two approaches rely on the initial formulation – which is strong or weak (variational) – and the implementation of the boundary conditions, that for the former include the continuity of stresses and displacements, whereas in the latter can consider the continuity of the displacements or both.

The two methodologies consider also a mapping technique to transform an element of general shape described in Cartesian coordinates into the same element in the computational space. Such technique can be implemented by employing the classic Lagrangian-shaped elements with a fixed number of nodes along the element edges or blending functions which allow an “exact mapping” of the element. In particular, the authors are employing NURBS (Not-Uniform Rational B-Splines) for such nonlinear mapping in order to use the “exact” shape of CAD designs.

**Keywords:** Structural analysis, Numerical methods, Strong formulation finite element method, Weak formulation finite element method, Differential and integral quadrature, Numerical stability and accuracy

### 1. Introduction

It is well-known that a physical phenomenon can be modeled by a system of differential equations, which are obtained once the proper hypotheses are introduced [1]-[4]. The solution of these complex differential equations cannot be reached analytically, thus a numerical method is needed for this purpose. This statement is especially true when a structural problem is taken into account, such as the vibrational or static behavior of laminated composite structures.

With reference to the papers by Tornabene et al. [5][6], it should be noted that the numerical approaches that can be employed in these circumstances are categorized according to the



formulation. In general, the solution of problem governed by a set of differential equations can be achieved by solving the strong or the weak form of the equations in hand. The governing equations are changed directly into a discrete system if the strong formulation is considered, since a numerical technique is introduced to approximate the derivatives. To this aim, different techniques can be used, such as some spectral methods for instance [7]-[9]. Among them, the Differential Quadrature (DQ) method should be mentioned due to its versatility and accuracy features [10]-[13]. A more stable and reliable approach was developed by Shu [14], and it is known in the literature as Generalized Differential Quadrature (GDQ) method. In this paper, only the main aspects of the DQ and GDQ techniques are presented. For the sake of completeness, the reader can find a more complete treatise about these methods in the review paper by Tornabene et al. [5].

On the other hand, the main aim of solving the weak formulation is to obtain an equivalent form of the governing equations by introducing a weighted-integral statement, which allows to reduce (or weaken) the order of differentiability of the differential equations. For this purpose, a numerical method able to compute integrals must be used. In the present paper, the Generalized Integral Quadrature (GIQ) is introduced to this aim [5][14]. Nevertheless, it should be mentioned that different weak form-based methods can be employed, as illustrated in the book by Reddy [4]. For the sake of completeness, it should be recalled that the weak form of the governing equations is solved also in the well-known Finite Element (FE) method [4][15].

In general, many practical applications require that the reference domain in which the governing equations are written is subdivided into several subdomains (or finite elements), due to the presence of geometric and mechanical discontinuities. At this point, a peculiar mapping technique can be developed to deal with arbitrarily shaped elements. Different approaches can be introduced for this purpose [16][17]. Recently, the theoretical framework provided by the Isogeometric Analysis (IGA) appears to be one of the most exploited approaches to study geometries with arbitrary edges [18][19]. Indeed, the use of blending functions based on NURBS (Non-Uniform Rational B-Splines) curves facilitates the analysis of generic domains. Both the domain decomposition and the mapping procedure are broadly used in classic FE method. Nevertheless, the same processes can be employed also when the strong form of the governing equations is considered [20]-[25]. The authors employ the names Strong Formulation Finite Element Method (SFEM) and Weak Formulation Finite Element Method (WFEM) to classify two different approaches based on the strong and weak forms of the governing equations, respectively.

In this paper, the accuracy, reliability and stability characteristics of SFEM and WFEM are discussed and compared by means of some numerical examples related to structural problems. A brief theoretical treatise is also presented for the sake of completeness. Further details concerning the structural models, as well as the governing equations, can be found in the works [26]-[30].

## **2. Numerical methods**

The main aspects of the numerical methods used in the computations are presented briefly in this section. In particular, the fundamentals of DQ are introduced firstly. Then, the corresponding technique used to approximate integrals is illustrated starting from the concepts employed for the numerical evaluation of derivatives.

### Approximation of derivatives

The derivative of a generic function can be approximated numerically by means of the DQ method. The key points of this technique are the evaluation of the weighting coefficients and the choice of a discrete distribution of grid points within the reference domain. Let us consider a one-dimensional function  $f(x)$  defined in the closed interval  $[a, b]$ . Such domain must be preventively discretized by placing  $I_N$  discrete grid points  $x_k \in [a, b]$ , according to the following relation

$$x_k = \frac{b-a}{d-c}(\zeta_k - c) + a \quad (1)$$

for  $k = 1, 2, \dots, I_N$ , where  $\zeta_k \in [c, d]$  denotes the points of a generic distributions. The most typical grid employed in many engineering problems are listed in Table 1, assuming

$$\zeta_k = \frac{r_k - r_1}{r_N - r_1} \quad (2)$$

where not specified. On the other hand, the basis polynomials required to evaluate the corresponding distribution will be indicated in the following. A more complete list of discrete grid distributions is presented in the books [31][32] and in the review paper by Tornabene et al. [5].

It should be recalled that a smooth function  $f(x)$  can be approximated by a set of basis functions  $\psi_j(x)$ , for  $j = 1, 2, \dots, I_N$ . From the mathematical point of view, one gets

$$f(x) \cong \sum_{j=1}^{I_N} \lambda_j \psi_j(x) \quad (3)$$

in which  $\lambda_j$  are unknown coefficients. By using a compact matrix form, Eq. (3) can be written as follows

$$\mathbf{f} = \mathbf{A}\boldsymbol{\lambda} \quad (4)$$

where  $\mathbf{f}$  represents the vector of the values that the function assumes in each grid point, whereas the vector  $\boldsymbol{\lambda}$  collects the terms  $\lambda_j$ . On the other hand,  $\mathbf{A}$  is the coefficient matrix, whose elements are given by  $A_{ij} = \psi_j(x_i)$ , for  $i, j = 1, 2, \dots, I_N$ . Since the unknown parameters  $\lambda_j$  do not depend on  $x$ , the  $n$ -th order derivative of  $f(x)$  can be computed as

$$\frac{d^n f(x)}{dx^n} = \sum_{j=1}^{I_N} \lambda_j \frac{d^n \psi_j(x)}{dx^n} \quad (5)$$

for  $n = 1, 2, \dots, I_N - 1$ . Analogously, a compact matrix form can be conveniently used

$$\mathbf{f}^{(n)} = \mathbf{A}^{(n)}\boldsymbol{\lambda} \quad (6)$$

where  $\mathbf{f}^{(n)}$  collects the values of the  $n$ -th order derivatives computed at each grid point. The coefficients of the matrix  $\mathbf{A}^{(n)}$  are clearly given by

$$A_{ij}^{(n)} = \frac{d^n \psi_j(x)}{dx^n} \Big|_{x_i} \quad (7)$$

for  $i, j = 1, 2, \dots, I_N$ . Having in mind Eq. (4), the unknown vector  $\lambda$  can be computed as

$$\lambda = \mathbf{A}^{-1} \mathbf{f} \quad (8)$$

Table 1. Grid point distributions. The symbol  $N$  denotes the total number of points

Unifor (Unif)	Chebyshev-Gauss-Lobatto (Cheb-Gau-Lob)
$\zeta_k = \frac{k-1}{N-1}, k = 1, 2, \dots, N$	$r_k = \cos\left(\frac{N-k}{N-1}\pi\right), k = 1, 2, \dots, N, r \in [-1, 1]$
Quadratic (Quad)	Chebyshev I kind (Cheb I)
$\left\{ \begin{array}{l} \zeta_k = 2\left(\frac{k-1}{N-1}\right)^2, k = 1, 2, \dots, \frac{N+1}{2} \\ \zeta_k = -2\left(\frac{k-1}{N-1}\right)^2 + 4\left(\frac{k-1}{N-1}\right) - 1, k = \frac{N+1}{2} + 1, \dots, N-1, N \end{array} \right.$	$r_k = \cos\left(\frac{2(N-k)+1}{2N}\pi\right), k = 1, 2, \dots, N, r \in [-1, 1]$
Chebyshev II kind (Cheb II)	Approximate Legendre (App Leg)
$r_k = \cos\left(\frac{N-k+1}{N+1}\pi\right), k = 1, 2, \dots, N, r \in [-1, 1]$	$r_k = \left(1 - \frac{1}{8N^2} + \frac{1}{8N^3}\right) \cos\left(\frac{4(N-k)+3}{4N+2}\pi\right),$ $k = 1, 2, \dots, N, r \in [-1, 1]$
Legendre-Gauss (Leg-Gau)	Radau I kind (Rad I)
$r_k = \text{roots of } (1-r^2)L_{N-1}(r), k = 1, 2, \dots, N, r \in [-1, 1]$	$r_k = \text{roots of } (1-r)(L_N(-r) + L_{N-1}(-r)),$ $k = 1, 2, \dots, N, r \in [-1, 1]$
Chebyshev-Gauss (Cheb-Gau)	Legendre-Gauss-Lobatto (Leg-Gau-Lob)
$r_1 = -1, r_N = 1, r_k = \cos\left(\frac{2(N-k)-1}{2(N-2)}\pi\right),$ $k = 2, 3, \dots, N-1, r \in [-1, 1]$	$r_k = \text{roots of } (1-r^2)A_{N-1}(r), k = 1, 2, \dots, N, r \in [-1, 1]$
Hermite (Her)	Laguerre (Lague)
$r_k = \text{roots of } H_{N+1}(r), k = 1, 2, \dots, N, r \in ]-\infty, +\infty[$	$r_k = \text{roots of } G_{N+1}(r), k = 1, 2, \dots, N, r \in [0, +\infty[$
Chebyshev-Gauss-Radau (Cheb-Gau-Rad)	Non uniform Ding (Ding)
$r_k = \cos\left(\frac{2(N-k)}{2N-1}\pi\right), k = 1, 2, \dots, N, r \in [-1, 1]$	$\zeta_k = \frac{1}{2}\left(1 - \sqrt{2} \cos\left(\frac{\pi}{4} + \frac{\pi}{2} \frac{k-1}{N-1}\right)\right), k = 1, 2, \dots, N$
Legendre (Leg)	Chebyshev III kind (Cheb III)
$r_k = \text{roots of } L_{N+1}(r), k = 1, 2, \dots, N, r \in [-1, 1]$	$r_k = \cos\left(\frac{2(N-k)+1}{2N+1}\pi\right), k = 1, 2, \dots, N, r \in [-1, 1]$
Chebyshev IV kind (Cheb IV)	Lobatto (Lob)
$r_k = \cos\left(\frac{2(N-k+1)}{2N+1}\pi\right), k = 1, 2, \dots, N, r \in [-1, 1]$	$r_k = \text{roots of } A_{N+1}(r), k = 1, 2, \dots, N, r \in [-1, 1]$
Legendre-Gauss-Radau (Leg-Gau-Rad)	Radau II kind (Rad II)
$r_k = \text{roots of } L_{N+1}(r) + L_N(r), k = 1, 2, \dots, N, r \in [-1, 1]$	$r_k = \text{roots of } (1-r)(L_N(r) + L_{N-1}(r)),$ $k = 1, 2, \dots, N, r \in [-1, 1]$
Jacobi (Jac)	Jacobi-Gauss (Jac-Gau)
$r_k = \text{roots of } J_{N-1}^{(\nu, \delta)}(r), k = 1, 2, \dots, N, r \in [-1, 1]$	$r_k = \text{roots of } (1-r^2)J_{N-1}^{(\nu, \delta)}(r), k = 1, 2, \dots, N, r \in [-1, 1]$

Thus, Eq. (8) allows to write the following definition

$$\mathbf{f}^{(n)} = \mathbf{A}^{(n)} \mathbf{A}^{-1} \mathbf{f} \quad (9)$$

According to the differentiation matrix procedure provided by the DQ method, the  $n$ -th order derivatives are given by

$$\mathbf{f}^{(n)} = \mathbf{D}^{(n)} \mathbf{f} \quad (10)$$

in which  $\mathbf{D}^{(n)}$  is the matrix that collects the so called weighting coefficients for the derivation. By comparing Eq. (9) and Eq. (10), it is evident that

$$\mathbf{D}^{(n)} = \mathbf{A}^{(n)} \mathbf{A}^{-1} \quad (11)$$

Therefore, it should be noted that the differentiation matrix  $\mathbf{D}^{(n)}$  can be computed as the matrix product between the matrix  $\mathbf{A}^{(n)}$  that collects the  $n$ -th order derivatives of the chosen basis functions at each discrete point of the domain and the inverse matrix of the operator  $\mathbf{A}$  that includes the values that the basis functions assume in every grid point. For completeness purpose, some of the basis functions that can be used for this purpose are listed in Table 2.

As highlighted in the review paper by Tornabene et al. [5], it is possible also to employ the well-known Radial Basis Functions (RBFs) for the functional approximation. Analogously, the same approximation can be achieved through the so-called Moving Least Squares (MLS) method [5]. For the sake of clarity, Eq. (10) assumes the following aspect

$$\left. \frac{d^n f(x)}{dx^n} \right|_{x_i} = \sum_{j=1}^{I_N} D_{ij}^{(n)} f(x_j) \quad (12)$$

for  $i = 1, 2, \dots, I_N$ , where  $D_{ij}^{(n)}$  denotes the elements collected in the differentiation matrix. It should be noted that Eq. (12) is analogous to the definition of numerical derivative provided by the Generalized Differential Quadrature (GDQ) method

$$\left. \frac{d^n f(x)}{dx^n} \right|_{x_i} = \sum_{j=1}^{I_N} \zeta_{ij}^{(n)} f(x_j) \quad (13)$$

where  $\zeta_{ij}^{(n)}$  are the weighting coefficients that can be collected in the corresponding matrix  $\zeta^{(n)}$ , so that one gets

$$\mathbf{f}^{(n)} = \zeta^{(n)} \mathbf{f} \quad (14)$$

Eq. (14) is equivalent to the definition shown in Eq. (10). The coefficients  $\zeta_{ij}^{(n)}$  can be computed by means of the recursive expressions provided by Shu [5], whereas a matrix multiplication and an inversion of a matrix are required to evaluate  $D_{ij}^{(n)}$ . It should be highlighted that the matrix  $\mathbf{A}$  could become ill-conditioned if the number of grid points  $I_N$  is increased, since it appears to be similar to the well-known Vandermonde matrix. It is proven that this problem happens for  $I_N > 13$ . It should be observed anyway that the number of discrete points is low when the reference domain is subdivided into finite elements, since the unknown field is well-approximated by using lower-order basis functions. However, the choice of particular basis functions such as Lagrange polynomials, Lagrange trigonometric polynomials, or the Sinc function, allows to overcome this issue since the coefficient matrix is

equal to the corresponding identity matrix (in other words, one gets  $\mathbf{A} = \mathbf{I}$ ). Thus, when the solution is obtained by using a single element, the unknown field requires higher-order basis functions for its approximation. Consequently, the numerical problems related to the ill-conditioned matrix can be avoided by choosing the aforementioned basis functions.

Table 2. Basis function employed for the functional approximation

Lagrange polynomials	Lagrange trigonometric polynomials
$\psi_j = l_j(r) = \frac{\mathcal{L}(r)}{(r-r_j)L^{(1)}(r_j)}, r \in ]-\infty, +\infty[, j = 1, 2, \dots, N$ $\mathcal{L}(r) = \prod_{k=1}^N (r-r_k), \mathcal{L}^{(1)}(r_j) = \prod_{k=1, k \neq j}^N (r_j - r_k)$	$\psi_j = g_j(r) = \frac{G(r)}{\sin\left(\frac{r-r_j}{2}\right)S^{(1)}(r_j)}, r \in [0, 2\pi], j = 1, 2, \dots, N$ $G(r) = \prod_{k=1}^N \sin\left(\frac{r-r_k}{2}\right), G^{(1)}(r_j) = \prod_{k=1, k \neq j}^N \sin\left(\frac{r_j-r_k}{2}\right)$
Bernstein polynomials	Lobatto polynomials
$\psi_j = B_j(r) = \frac{(N-1)!}{(j-1)!(N-j)!} r^{j-1} (1-r)^{N-j}$ $r \in [0, 1], j = 1, 2, \dots, N$	$\psi_j = A_j(r) = \frac{d}{dr}(L_{j+1}(r)), r \in [-1, 1], j = 1, 2, \dots, N$
Exponential functions	Monomial polynomials
$\psi_j = E_j(r) = e^{(j-1)r}, r \in ]-\infty, +\infty[, j = 1, 2, \dots, N$	$\psi_j = Z_j(r) = r^{j-1}, r \in ]-\infty, +\infty[, j = 1, 2, \dots, N$
Bessel polynomials	Sinc functions
$\psi_1 = P_1(r) = 1, \psi_j = P_j(r) = \sum_{k=0}^{j-1} \frac{(j-1+k)!}{(j-1-k)!k!} \left(\frac{r}{2}\right)^k$ $r \in [-\infty, +\infty], j = 2, 3, \dots, N$	$\psi_j = S_j = \text{Sinc}_j(r) = \frac{\sin(\pi(N-1)(r-r_j))}{\pi(N-1)(r-r_j)}$ $r \in [0, 1], j = 1, 2, \dots, N$
Fourier functions	Boubaker polynomials
$\psi_1 = F_1(r) = 1, \psi_j = F_j(r) = \cos\left(\frac{j}{2}r\right) \text{ for } j \text{ even}$ $\psi_j = F_j(r) = \sin\left(\frac{j-1}{2}r\right) \text{ for } j \text{ odd}$ $r \in [0, 2\pi], j = 2, 3, \dots, N$	$\psi_1 = Q_1(r) = 1, r \in [-\infty, +\infty], j = 2, 3, \dots, N$ $\psi_j = Q_j(r) = \sum_{k=0}^{\phi(j-1)} (-1)^k \binom{j-1-k}{k} \frac{j-1-4k}{j-1-k} r^{j-1-2k}$ $\phi(j-1) = \frac{2(j-1) + ((-1)^{j-1} - 1)}{4}$
Jacobi Polynomials	Legendre polynomials
$\psi_j = J_j^{(\gamma, \delta)}(r) = \frac{(-1)^{j-1}}{2^{j-1}(j-1)!(1-r)^\gamma(1+r)^\delta} \frac{d^{j-1}}{dr^{j-1}}((1-r)^{j-1+\gamma}(1+r)^{j-1+\delta})$ $r \in [-1, 1], j = 1, 2, \dots, N, \gamma, \delta > -1$	$\psi_j = L_j(r) = \frac{(-1)^{j-1}}{2^{j-1}(j-1)!} \frac{d^{j-1}}{dr^{j-1}}((1-r^2)^{j-1})$ $r \in [-1, 1], j = 1, 2, \dots, N$
Chebyshev polynomials (I kind)	Chebyshev polynomials (II kind)
$\psi_j = T_j(r) = \cos((j-1)\arccos(r)), r \in [-1, 1], j = 1, 2, \dots, N$	$\psi_j = U_j(r) = \frac{\sin(j \arccos(r))}{\sin(\arccos(r))}, r \in [-1, 1], j = 1, 2, \dots, N$
Chebyshev polynomials (III kind)	Chebyshev polynomials (IV kind)
$\psi_j = V_j(r) = \frac{\cos\left(\frac{(2j-1)\arccos(r)}{2}\right)}{\cos\left(\frac{\arccos(r)}{2}\right)}, r \in [-1, 1], j = 1, 2, \dots, N$	$\psi_j = W_j(r) = \frac{\sin\left(\frac{(2j-1)\arccos(r)}{2}\right)}{\sin\left(\frac{\arccos(r)}{2}\right)}, r \in [-1, 1], j = 1, 2, \dots, N$
Laguerre polynomials	Hermite polynomials
$\psi_j = G_j(r) = \frac{1}{(j-1)!} \frac{d^{j-1}}{dr^{j-1}}(r^{j-1}e^{-r}), r \in [0, +\infty[, j = 1, 2, \dots, N$	$\psi_j = H_j(r) = (-1)^{j-1} e^{r^2} \frac{d^{j-1}}{dr^{j-1}}(e^{-r^2}), r \in ]-\infty, +\infty[, j = 1, 2, \dots, N$



$$\mathbf{C}_x^{(n)} = \mathbf{I} \otimes \mathbf{D}_x^{(n)} \quad (17)$$

$(I_N \cdot I_M) \times (I_N \cdot I_M)$      $I_M \times I_M$      $I_N \times I_N$

$$\mathbf{C}_y^{(m)} = \mathbf{D}_y^{(m)} \otimes \mathbf{I} \quad (18)$$

$(I_N \cdot I_M) \times (I_N \cdot I_M)$      $I_M \times I_M$      $I_N \times I_N$

$$\mathbf{C}_{xy}^{(n+m)} = \mathbf{D}_y^{(m)} \otimes \mathbf{D}_x^{(n)} \quad (19)$$

$(I_N \cdot I_M) \times (I_N \cdot I_M)$      $I_M \times I_M$      $I_N \times I_N$

in which  $\mathbf{I}$  represents the identity matrix, whereas  $\mathbf{D}_x^{(n)}, \mathbf{D}_y^{(m)}$  collect the weighting coefficients along the two principal coordinates, which can be evaluated as shown above. The size of every operator is indicated under the corresponding matrix for the sake of completeness. Once the weighting coefficients related to the current scheme are computed and collected in the corresponding matrices  $\mathbf{C}_x^{(n)}, \mathbf{C}_y^{(m)}, \mathbf{C}_{xy}^{(n+m)}$ , the derivatives of the considered function are given by the following matrix products

$$\mathbf{f}_x^{(n)} = \mathbf{C}_x^{(n)} \mathbf{f} \quad (20)$$

$$\mathbf{f}_y^{(m)} = \mathbf{C}_y^{(m)} \mathbf{f} \quad (21)$$

$$\mathbf{f}_{xy}^{(n+m)} = \mathbf{C}_{xy}^{(n+m)} \mathbf{f} \quad (22)$$

In particular,  $\mathbf{f}_x^{(n)}$  collects the  $n$ -th order derivatives with respect to  $x$ ,  $\mathbf{f}_y^{(m)}$  is the vector of the  $m$ -th order derivatives with respect to  $y$ , whereas  $\mathbf{f}_{xy}^{(n+m)}$  represents  $(n+m)$ -th order mixed derivatives. The size of all these vectors, as well as of  $\mathbf{f}$ , is given by  $(I_N \cdot I_M) \times 1$ .

At this point, it should be mentioned that the present approach is used to obtain and solve the strong form of the governing equations. If a subdivision of the reference domain into finite elements is required, the technique is termed Strong Formulation Finite Element Method (SFEM). It is clear that the vector  $\mathbf{f}$  denotes the unknown field of the partial differential equations of the fundamental system, which is transformed directly into a system of discrete equations by means of the DQ method.

### Approximation of integrals

Starting from the ideas and definitions illustrated for the numerical evaluation of derivatives, a numerical scheme for the computation of integrals can be developed. In this section, the main aspects of this integral quadrature are presented briefly. Since the Lagrange polynomials are used as basis functions for the functional approximation, the technique at issue is known in the literature as Generalized Integral Quadrature (GIQ). Nevertheless, it should be recalled that different basis functions can be chosen for the same purpose.

Let us consider the same one-dimensional function  $f(x)$  defined in the closed interval  $[a, b]$  introduced in the previous section. As shown in Eq. (1), the reference domain is discretized so that one gets  $x_k \in [a, b]$ . All the grid distributions listed in Table 1 could be employed. By definition, the integral of  $f(x)$  within the closed interval  $[x_i, x_j]$ , with  $x_i, x_j \in [a, b]$ , can be approximated as follows

$$\int_{x_i}^{x_j} f(x) dx = \sum_{k=1}^{I_N} w_k^{ij} f(x_k) \quad (23)$$

where  $I_N$  denotes the total number of discrete points, whereas  $w_k^{ij}$  are the weighting coefficients for the integration. It should be noted that the numerical integration in Eq. (23) requires to consider all the sampling points of the domain independently from the integration limits. Eq. (23) becomes a conventional integral for  $x_i = a$  and  $x_j = b$ . In order to evaluate the weighting coefficients, the following quantities must be introduced

$$\begin{aligned}\bar{\zeta}_{ij}^{(1)} &= \frac{x_i - c}{x_j - c} \zeta_{ij}^{(1)} \quad \text{for } i \neq j \\ \bar{\zeta}_{ij}^{(1)} &= \zeta_{ii}^{(1)} + \frac{1}{x_i - c} \quad \text{for } i = j\end{aligned}\tag{24}$$

for  $i=1,2,\dots,I_N$ . It is clear that  $\zeta_{ij}^{(1)}$  stands for the weighting coefficients for the first-order derivatives, computable through the recursive formulae provided by Shu as explained in the previous section. The arbitrary constant  $c$  should be set equal to  $c = b + 10^{-10}$  to guarantee the accuracy and stability of the numerical solution. The coefficients introduced in Eq. (24) can be collected in the corresponding matrix  $\bar{\zeta}^{(1)}$  of size  $I_N \times I_N$ . At this point, this last matrix must be inverted as follows to obtain the matrix of the weighting coefficients for the integration

$$\mathbf{W} = \left( \bar{\zeta}^{(1)} \right)^{-1}\tag{25}$$

A generic term of  $\mathbf{W}$  is specified by the notation  $w_{ij}$ , for  $i, j=1,2,\dots,I_N$ . Finally, the weighting coefficients  $w_k^{ij}$  needed in Eq. (23) are given by

$$w_k^{ij} = w_{jk} - w_{ik}\tag{26}$$

for  $k=1,2,\dots,I_N$ . These  $I_N$  coefficients can be conveniently collected in a row vector  $\mathbf{W}_x$ , whose size is  $1 \times I_N$ . In compact matrix form, the numerical integral  $I$  is computed as a vector product

$$I = \mathbf{W}_x \mathbf{f}\tag{27}$$

If the integration limits are set equal to  $x_i = a$  and  $x_j = b$ , or in other words  $x_i = x_1$  and  $x_j = x_{I_N}$ , the numerical integration can be performed by using the weighting coefficients  $w_k^{I_N}$ , which are defined as follows

$$w_k^{I_N} = w_{I_N k} - w_{1k}\tag{28}$$

A transformation of these weighting coefficients must be performed to switch from the reference interval  $[\alpha, \beta]$  to a generic one  $[a, b]$ . The weighting coefficients  $w_k^{I_N}$  in the physical interval  $[a, b]$  are given by

$$w_k^{I_N} = \frac{b-a}{\beta-\alpha} \tilde{w}_k^{I_N}\tag{29}$$

where  $\tilde{w}_k^{I_N}$  represents the weighting coefficients related to the shifted interval  $[\alpha, \beta]$ . It is important to underline that this approach can be applied without any restriction on the grid point distributions employed to discretize the reference domain.

As shown above, the two-dimensional counterpart can be easily deduced. Let us consider a generic smooth function  $f(x, y)$  defined in a two-dimensional domain, where the main coordinates  $x, y$  are given by  $x \in [a, b]$  and  $y \in [c, d]$ . The numerical integral performed in the whole domain is defined as follows

$$\int_c^d \int_a^b f(x, y) dx dy = \sum_{i=1}^{I_N} \sum_{j=1}^{I_M} w_i^{I_N} w_j^{I_M} f(x_i, y_j) \quad (30)$$

in which the weighting coefficients  $w_i^{I_N}, w_j^{I_M}$  can be evaluated by applying the same procedure just illustrated along the two principal coordinates. In order to facilitate the implementation process, these coefficients can be collected in the corresponding vectors denoted by  $\mathbf{W}_x, \mathbf{W}_y$ , respectively. Even in this circumstance, the same scheme used before to order the grid points should be used (Figure 1). By using the Kronecker product, the vector of the weighting coefficients for the two-dimensional integration is obtained

$$\mathbf{W}_{xy} = \mathbf{W}_y \otimes \mathbf{W}_x \quad (31)$$

$1 \times (I_N \cdot I_M) \quad 1 \times I_M \quad 1 \times I_N$

A simple matrix product is required to evaluate the numerical integration shown in Eq. (30). Analogously to the one-dimensional scheme, the integral  $I$  is given by

$$I = \mathbf{W}_{xy} \mathbf{f} \quad (32)$$

where  $\mathbf{f}$  assumes the meaning shown in Eq. (16). The current approach is employed to obtain and solve the weak form of the governing equations. When the reference domain is decomposed into finite elements, the technique in hand is named Weak Formulation Finite Element Method (WFEM).

### 3. Applications

In this section, some applications related to the structural analysis of plates and shells are presented. Both the strong and weak formulations are employed and the numerical results are obtained by using different basis functions and grid distributions.

#### *Isotropic plates*

The numerical tests shown in this paragraph are related to the convergence analysis of simply-supported plates in terms of the first circular frequency  $\omega_1$ . The reference solution  $\omega_{1ex}$  for this structure is shown in the review paper by Tornabene et al. [5]. The square plates of side  $L=1\text{m}$  and thickness  $h=0.1\text{m}$  are made of isotropic material ( $E=70\text{GPa}$ ,  $\nu=0.3$ ,  $\rho=2707\text{kg/m}^3$ ). In the first applications, the two formulations are employed by varying grid distributions and basis functions in the theoretical framework provided by the Reissner-Mindlin theory, increasing the number of grid points  $I_N = I_M = N$ . The structural model is composed by a sole element due to its regular shape. Figure 2 and Figure 3 show the convergence analyses for the weak and strong formulations, respectively. It is easy to note

that some grid distributions do not provide accurate results. This aspect is even more evident for the strong formulation (Figure 3). In general, the solutions converge by using a reduced number of points ( $N = 11 \div 15$ ). On the other hand, the MLS method gives inaccurate results, especially for the weak form. For this technique, the Gaussian quadric function is used as basis function.

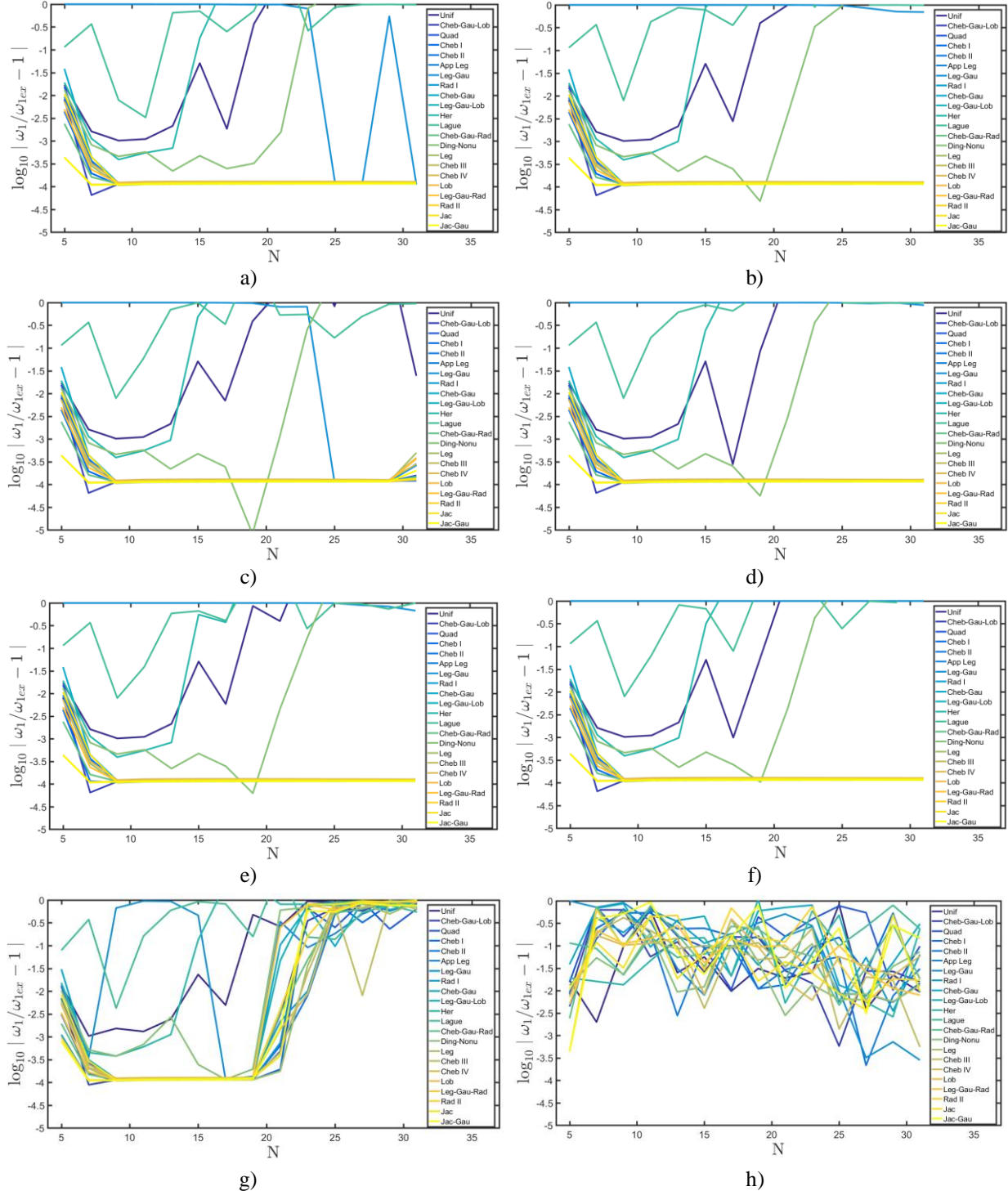


Fig. 2. Relative error for the first frequency of a simply-supported square plate. The weak formulation is employed considering different basis functions: a) Bernstein polynomials; b) Bessel polynomials; c) Boubaker polynomials; d) Chebyshev (I kind) polynomials; e) Exponential functions; f) Lagrange polynomials; g) Fourier basis functions; h) MLS method (Gaussian quadric basis functions)

A second set of convergence analyses is performed considering an isotropic rectangular plate ( $L_x = 2\text{m}$ ,  $L_y = 1.5\text{m}$ ,  $h = 0.1\text{m}$ ) characterized by the same mechanical properties and boundary conditions of the previous tests.

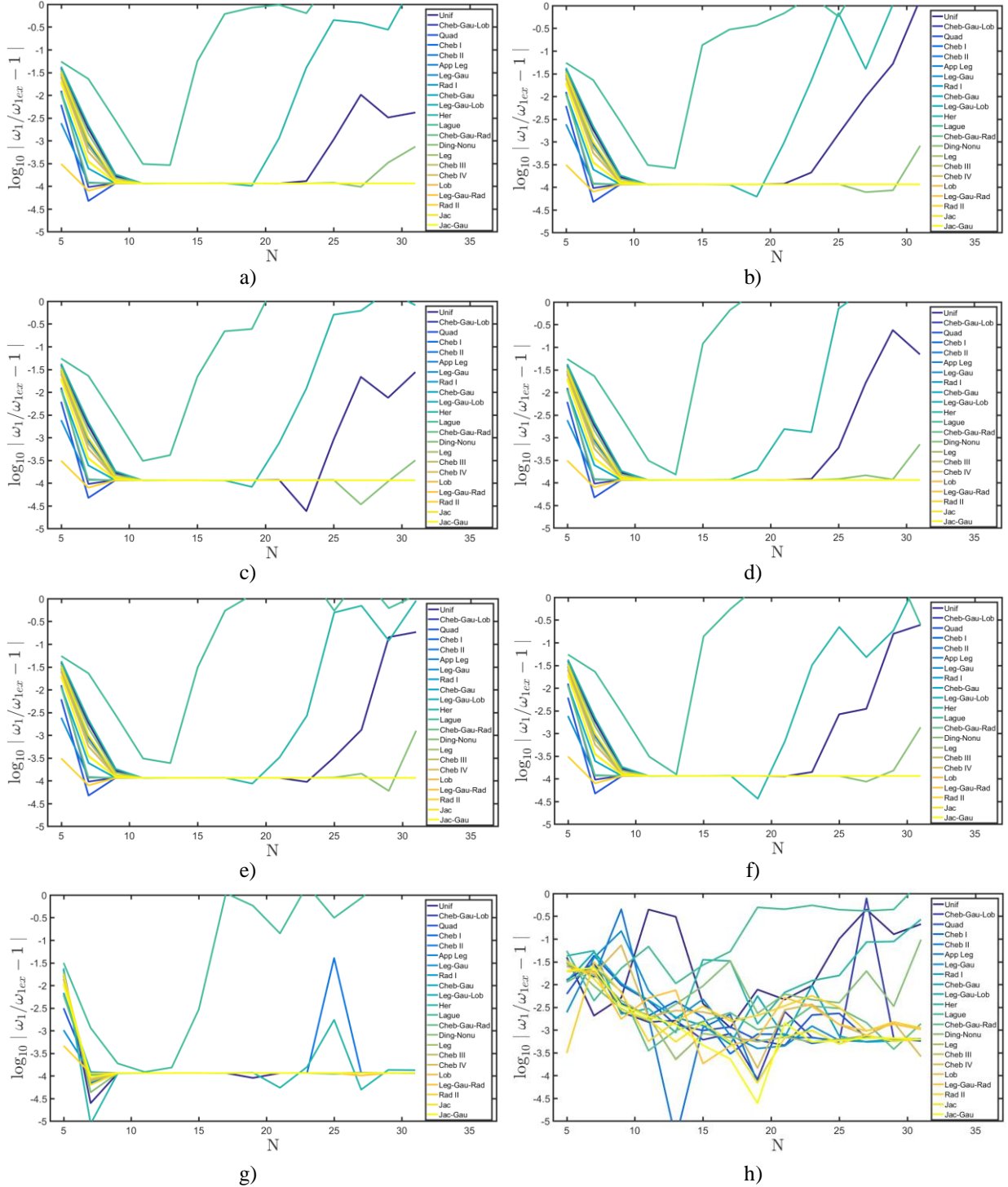


Fig. 3. Relative error for the first frequency of a simply-supported square plate. The strong formulation is employed considering different basis functions: a) Bernstein polynomials; b) Bessel polynomials; c) Boubaker polynomials; d) Chebyshev (I kind) polynomials; e) Exponential functions; f) Lagrange polynomials; g) Fourier basis functions; h) MLS method (Gaussian quadric basis functions)

If  $f_{ref}$  denotes the reference solution in term of natural frequency, the relative error is

$$\varepsilon = \frac{f_n}{f_{ref}} - 1 \quad (33)$$

where  $n$  stands for the considered vibration mode. For the sake of completeness, the Navier type solution can be found in [5]. The same analyses are performed by means of two finite element commercial codes (Strand7 and Abaqus) by using several kinds of plate elements, as specified in Table 3. A complete description of these elements can be found in the corresponding documentation of the software.

Table 3. Finite elements available in the commercial codes used in the computations

<b>Strand7</b>		
Quadrangular	Triangular	
<i>Quad4</i> (4 nodes)	<i>Tri3</i> (3 nodes)	
<i>Quad8</i> (8 nodes)	<i>Tri6</i> (6 nodes)	
<i>Quad9</i> (9 nodes)	-	
<b>Abaqus</b>		
General purpose	Thin structures	Thick structures
<i>S4</i> (quadrangular, 4 nodes)	<i>S8R5</i> (quadrangular, 8 nodes)	<i>S8R</i> (quadrangular, 8 nodes)
<i>S4R</i> (quadrangular, 4 nodes)	<i>STRI65</i> (triangular, 6 nodes)	-
<i>S3</i> (triangular, 3 nodes)	-	-

As far as the present approaches are concerned, the strong formulation is used with the Cheb-Gau-Lob (CGL) grid, whereas the Leg-Gau-Lob (LGL) is employed for the weak form. The Lagrange polynomials are employed for both the formulations. In this example, the reference domain is divided into elements and the notations SFEM $_j$  and WFEM $_j$  are introduced. The symbol  $j$  stands for the number of elements ( $j = 1, 2, 4, 8, 16$ ) used for the computation. The results are shown in Figure 4 for the first three mode shapes of the isotropic rectangular plate, where the relative error is given as a function of the degrees of freedom of the problem ( $DOFS$ ). It can be observed that the present approaches show a rapid convergence if compared to the commercial codes, independently from the number of finite elements. Thus, the current approaches require a reduced number of degrees of freedom to obtain accurate results. The strong and the weak based methodologies are characterized by the same level of accuracy, when the corresponding structural models are considered. It is important to note that both the SFEM and WFEM are able to capture the reference solutions and the machine epsilon is reached. This aspect is highlighted by the horizontal lines in the graphs of Figure 4. Finally, it should be specified that the theoretical model is provided by the Reissner-Mindlin theory [25].

#### Laminated plates

The same structure is considered in this paragraph to perform the convergence analyses for a laminated plate, whose stacking sequence is given by (90/0/90/0/90). The orthotropic mechanical properties are the following ones

$$\begin{aligned} E_1 = 137.9 \text{ GPa}, \quad E_2 = E_3 = \frac{E_1}{40}, \quad G_{12} = G_{13} = 0.6E_2, \\ G_{23} = 0.6E_2, \quad \nu_{12} = \nu_{13} = \nu_{23} = 0.25, \quad \rho = 1450 \text{ kg/m}^3 \end{aligned} \quad (34)$$

As shown above, the results are given in terms of the relative error (33) related to the Navier solution specified in [5], for the Reissner-Mindlin theory. The notations and considerations of these tests are the same of the previous application. The convergence graphs are depicted in Figure 5.

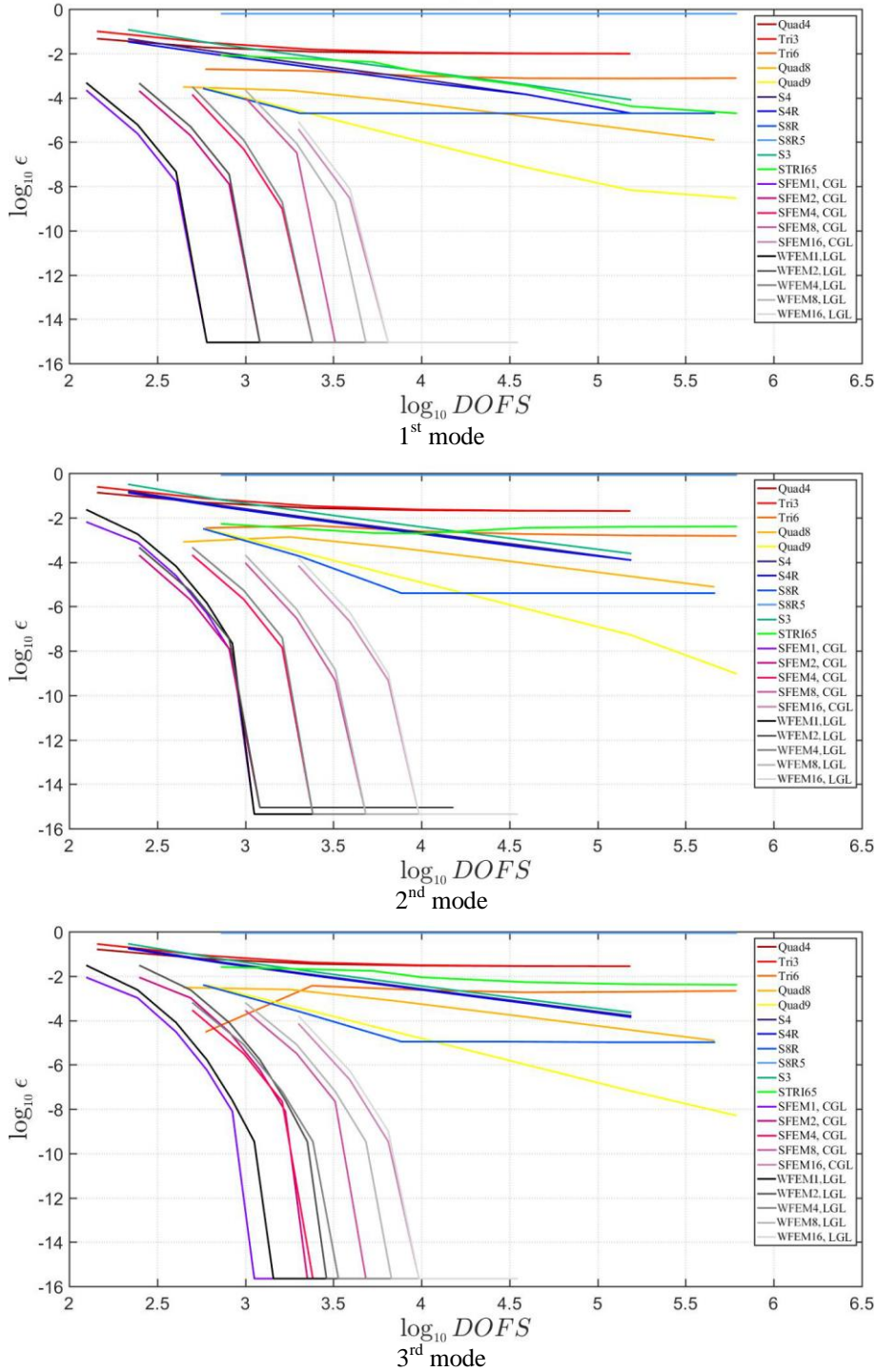


Fig. 4. Relative error for the first three natural frequencies of a simply-supported isotropic rectangular plate increasing the number of degrees of freedom ( $DOFS$ ). Both the strong and weak formulations are employed by dividing the domain into finite elements. The present solutions are compared with the ones obtained by different models obtained through several plate elements provided by two finite element commercial codes.

It should be noted that the machine epsilon is reached in each model for the present solution. On the other hand, the accuracy of the commercial codes is decreased if compared to the corresponding isotropic case.

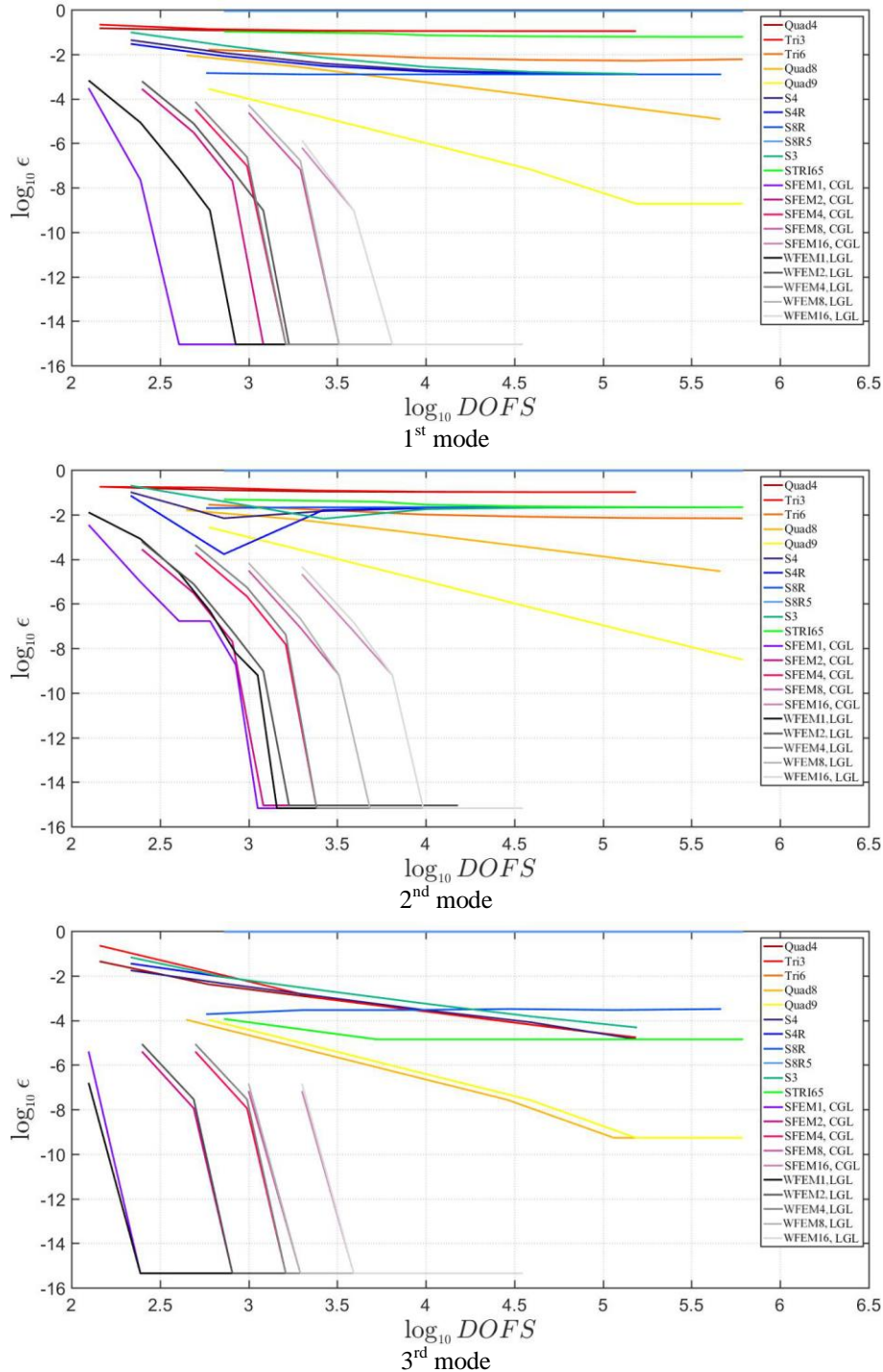


Fig. 5. Relative error for the first three natural frequencies of a simply-supported laminated rectangular plate increasing the number of degrees of freedom ( $DOFS$ ). Both the strong and weak formulations are employed by dividing the domain into finite elements. The present solutions are compared with the ones obtained by different models obtained through several plate elements provided by two finite element commercial codes.

In the applications just presented there is no need of a mapping procedure, since the domain has a regular shape. In the following, a fully clamped circular plate of radius  $R=1$  m and thickness  $h$  is analyzed. The lamination scheme is given by (30/45) and the two layers have the properties shown in (34) and the same thickness. The convergence analyses are shown in Figure 6 for two ratios  $R/h$  to deal with thick and thin structures, respectively.

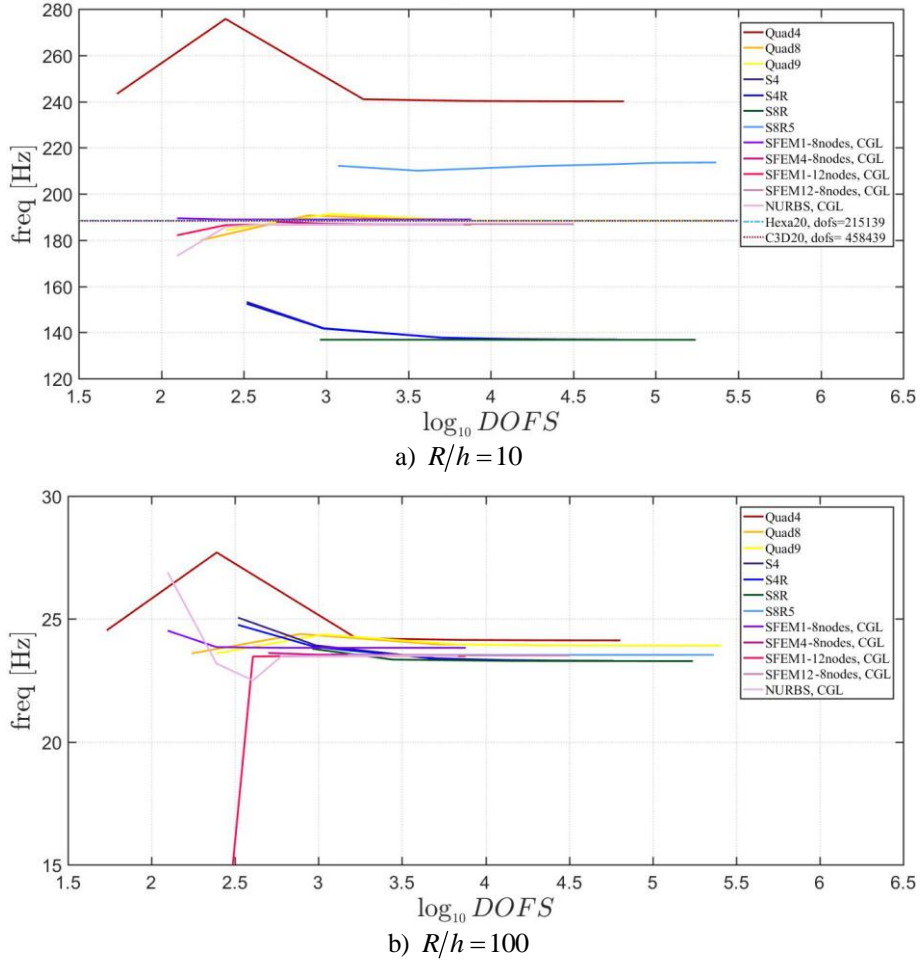


Fig. 6. First natural frequency for a fully clamped laminated circular plate increasing the number of degrees of freedom ( $DOFS$ ), for two different thickness values: a)  $R/h = 10$  ; b)  $R/h = 100$

As shown above, several kinds of plate elements are considered when the solutions are obtained by means of the finite element commercial codes. As far as the present approach is concerned, only the strong formulation is solved by using different element configurations, as specified in the legend of the corresponding graphs, where the number of nodes required for the mapping of the curved edges of the structure is indicated too. An isogeometric mapping based on NURBS curves is also implemented and compared with the other results. Only for the thicker case, a three-dimensional finite element solution (achieved by means of Strand7 and Abaqus) is computed and taken as a reference. These models are obtained through brick elements made of 20 nodes, named Hexa20 and C3D20 respectively. Both the SFEM and NURBS graphs tend to this solution with a reduced number of degrees of freedom. On the other hand, some types of elements provide convergence plots that are considerably detached from the reference ones, since they are not suitable to deal with this particular problem. Indeed, a similar tendency is achieved by means of each element for the thin plate. Finally, it

should be specified that the solutions are obtained in the framework of the Reissner-Mindlin theory.

*Laminated shells*

The last example is focused on the free vibration analysis of a doubly-curved laminated translational shell made of two orthotropic layers of equal thickness, whose geometry is widely described in the paper by Tornabene et al. [26]. The stacking sequence is given by (30/45), and their mechanical properties are the following ones

$$\begin{aligned} E_1 = 137.9 \text{ GPa}, E_2 = E_3 = 8.96 \text{ GPa}, G_{12} = G_{13} = 7.1 \text{ GPa}, \\ G_{23} = 6.21 \text{ GPa}, \nu_{12} = \nu_{13} = 0.3, \nu_{23} = 0.49, \rho = 1450 \text{ kg/m}^3 \end{aligned} \quad (35)$$

The overall thickness is assumed as  $h = 0.1 \text{ m}$ . In this case, the first ten natural frequencies are obtained by solving only the weak formulation of the governing equations. A unified formulation is used to deal with higher-order shear deformation theories, as illustrated in the paper [30], where the reader can find a complete treatise about these structural models, as well as the nomenclature to denote them. The Leg-Gau-Lob grid distribution is employed by setting  $I_N = 30$  and  $I_M = 60$  as number of discrete points along the two principal directions. The first ten natural frequencies are presented in Table 4, together with the reference solution obtained by Abaqus (three-dimensional finite element model). All the numerical solutions are in good agreement with the reference one. For the sake of completeness, the first three mode shapes are depicted in Figure 7, where it is easy to note also the adopted boundary conditions. In particular, only one of the two external edges is fully clamped, whereas the other one is free.

Table 4. First ten frequencies for a doubly-curved laminated panel

Mode [Hz]	FSDT	TSDT	ED1	ED2	ED3	3D FEM Abaqus
$f_1$	21.808	21.821	22.134	21.798	21.826	21.811
$f_2$	22.323	22.347	22.388	22.186	22.207	22.205
$f_3$	22.576	22.589	22.883	22.557	22.584	22.566
$f_4$	33.055	33.089	33.013	32.824	32.857	32.854
$f_5$	43.251	43.287	43.622	43.053	43.109	43.085
$f_6$	44.870	44.874	45.932	44.957	45.027	44.986
$f_7$	45.641	45.641	46.774	45.754	45.832	45.783
$f_8$	52.459	52.489	52.837	52.251	52.308	52.263
$f_9$	54.176	54.186	54.694	54.570	54.571	54.561
$f_{10}$	64.235	64.258	64.290	64.001	64.039	64.006

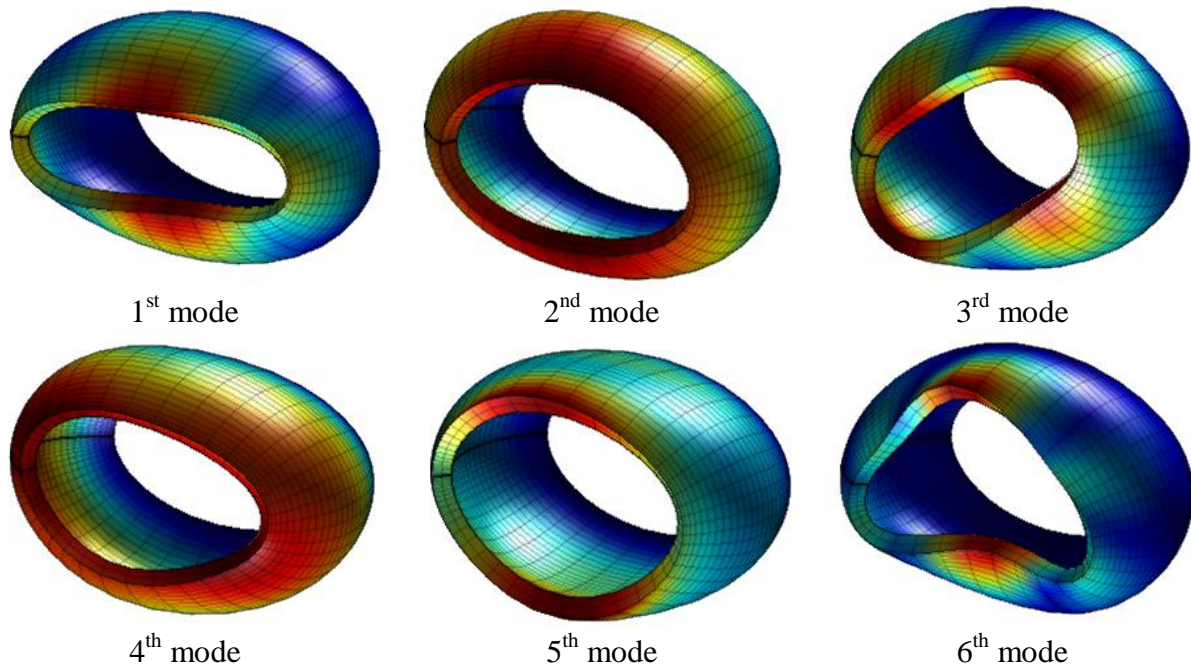


Fig. 7. First six mode shapes for a doubly-curved laminated shell of translation

#### 4. Conclusions

The authors have presented two numerical approaches based on the DQ method to approximate derivatives and integrals, respectively. These techniques have been applied to solve some structural problems related to the mechanical behavior of plates and shells made of isotropic and composite materials. In particular, the accuracy and stability features of a strong formulation (SFEM) and a weak formulation (WFEM) have been discussed by means of some numerical analyses. Several basis polynomials for the functional approximation and different discrete grid distributions have been tested and compared. For this purpose, some convergence analyses have been performed by increasing the number of sampling points within the elements, for both a single element domain and a multi-element domain. The present solutions have been compared also with the results obtained through two commercial codes. These finite element models have been achieved by using several kinds of plate elements available in the software libraries. In general, the present methodologies have proven to be more accurate and characterized by a faster convergence ratio than the commercial codes.

#### Acknowledgements

The research topic is one of the subjects of the Centre of Study and Research for the Identification of Materials and Structures (CIMEST)-“M. Capurso” of the University of Bologna (Italy).

#### References

- [1] Oden, J.T., and Reddy, J.N., *An introduction to the mathematical theory of finite elements*, John Wiley & Sons, 1976.

- [2] Ochoa, O.O. and Reddy, J.N., *Finite Element Analysis of Composite Laminates*, Springer, 1992.
- [3] Zienkiewicz, O.C. and Taylor R.L., *The Finite Element Method for Solid and Structural Mechanics*, 6<sup>th</sup> edition, Elsevier, 2005.
- [4] Reddy, J.N., *An introduction to the finite element method*, 3<sup>rd</sup> edition, McGraw-Hill, 2006.
- [5] Tornabene, F., Fantuzzi, N., Ubertini, F. and Viola, E., Strong Formulation Finite Element Method Based on Differential Quadrature: A Survey, *Applied Mechanics Reviews*, 67, 020801-1-55, 2015.
- [6] Tornabene, F., Fantuzzi, N., and Baccocchi, M., The Strong Formulation Finite Element Method: Stability and Accuracy, *Fracture and Structural Integrity*, 29, 251-265, 2014.
- [7] Gottlieb, D., and Orszag, S.A., *Numerical Analysis of Spectral Methods: Theory and Applications*, CBMS-NSF Regional Conference Series in Applied Mathematics., SIAM, 1977.
- [8] Boyd, J.P., *Chebyshev and Fourier Spectral Methods*, Dover Publications, 2001.
- [9] Canuto, C., Hussaini, M.Y., Quarteroni, A., and Zang, T.A., *Spectral Method. Fundamentals in Single Domains*, Springer, 2006.
- [10] Bellman, R., and Casti, J., Differential quadrature and long-term integration, *Journal of Mathematical Analysis and Applications*, 34, 235-238, 1971.
- [11] Bert, C.W., and Malik, M., Differential quadrature method in computational mechanics, *Applied Mechanics Reviews*, 49, 1-27, 1996.
- [12] Quan, J.R., and Chang, C.T., New insights in solving distributed system equations by the quadrature method - I. Analysis, *Computers & Chemical Engineering*, 13, 779-788, 1989.
- [13] Striz, A.G., Chen, W.L., and Bert, C.W., Static analysis of structures by the quadrature element method (QEM), *International Journal of Solids and Structures*, 31, 2807-2818, 1994.
- [14] Shu, C., *Differential Quadrature and Its Application in Engineering*, Springer, 2000.
- [15] Reddy, J.N., *Mechanics of Laminated Composites Plates and Shells*, 2<sup>nd</sup> edition, CRC Press, New York, 2004.
- [16] Chen, C.-N., *Discrete Element Analysis Methods of Generic Differential Quadratures*, Springer, 2006.

- [17] Zong, Z., and Zhang, Y.Y., *Advanced Differential Quadrature Methods*, CRC Press, 2009.
- [18] Cottrell, J.A., Hughes, T.J.R. and Bazilevs, Y., *Isogeometric Analysis. Toward Integration of CAD and FEA*, John Wiley & Sons, 2009.
- [19] Reali, A., An isogeometric analysis approach for the study of structural vibrations, *Journal of Earthquake Engineering*, 10, 1-30, 2006.
- [20] Tornabene, F., Fantuzzi, N. and Baccocchi M., The GDQ Method for the Free Vibration Analysis of Arbitrarily Shaped Laminated Composite Shells Using a NURBS-Based Isogeometric Approach, *Composite Structures*, 154, 190-218, 2016.
- [21] Fantuzzi, N. and Tornabene F., Strong Formulation Isogeometric Analysis (SFIGA) for Laminated Composite Arbitrarily Shaped Plates, *Composites Part B Engineering* 96, 173-203, 2016.
- [22] Viola, E., Tornabene, F. and Fantuzzi N., Generalized Differential Quadrature Finite Element Method for Cracked Composite Structures of Arbitrary Shape, *Composite Structures*, 106, 815-834, 2013.
- [23] Fantuzzi, N., Baccocchi, M., Tornabene, F., Viola, E. and Ferreira, A.J.M., Radial Basis Functions Based on Differential Quadrature Method for the Free Vibration of Laminated Composite Arbitrary Shaped Plates, *Composites Part B Engineering* 78, 65-78, 2015.
- [24] Tornabene, F., Fantuzzi, N., Baccocchi, M., Neves, A.M.A. and Ferreira, A.J.M., MLS-DQ Based on RBFs for the Free Vibrations of Laminated Composite Doubly-Curved Shells, *Composites Part B: Engineering* 99, 30-47, 2016.
- [25] Fantuzzi, N., Tornabene, F., Baccocchi, M., Neves, A.M.A. and A.J.M. Ferreira, Stability and Accuracy of Three Fourier Expansion-Based Strong Form Finite Elements for the Free Vibration Analysis of Laminated Composite Plates, *International Journal for Numerical Methods in Engineering* (in press), 2017.
- [26] Tornabene, F., Fantuzzi, N. and Baccocchi, M., The local GDQ method applied to general higher-order theories of doubly-curved laminated composite shells and panels: The free vibration analysis, *Composite Structures*, 116, 637-660, 2014.
- [27] Tornabene, F., Brischetto, S., Fantuzzi, N., and Baccocchi M., Boundary Conditions in 2D Numerical and 3D Exact Models for Cylindrical Bending Analysis of Functionally Graded Structures, *Shock and Vibration Vol.* 2016, Article ID 2373862, 1-17, 2016.

- [28]Tornabene, F., Fantuzzi, N., Baccocchi, M. and Reddy J.N., An Equivalent Layer-Wise Approach for the Free Vibration Analysis of Thick and Thin Laminated Sandwich Shells, *Applied Sciences*, 7, 17, 1-34, 2017.
- [29]Brischetto, S., Tornabene, F., Fantuzzi, N. and Baccocchi, M., Interpretation of Boundary Conditions in the Analytical and Numerical Shell Solutions for Mode Analysis of Multilayered Structures, *International Journal of Mechanical Sciences*, 122, 18-28, 2017.
- [30]Tornabene, F., Fantuzzi, N., Baccocchi, M., Viola, E. and Reddy J.N., A Numerical Investigation on the Natural Frequencies of FGM Sandwich Shells with Variable Thickness by the Local Generalized Differential Quadrature Method, *Applied Sciences*, 7, 131, 1-39, 2017.
- [31]Tornabene, F., Fantuzzi, N., Baccocchi, M. and Viola, E., *Laminated Composite Doubly-Curved Shell Structures. Differential Geometry. Higher-Order Structural Theories*, Esculapio, 2016.
- [32]Tornabene, F., Fantuzzi, N., Baccocchi, M. and Viola, E., *Laminated Composite Doubly-Curved Shell Structures. Differential and Integral Quadrature. Strong Formulation Finite Element Method*, Esculapio, 2016.